Ice flow-unit influence on glacier structure, debris entrainment and transport

Jennings, Stephen J. A.; Hambrey, Michael J.; Glasser, Neil F.

Published in:
Earth Surface Processes and Landforms

DOI:
10.1002/esp.3521

Publication date:
2014

Citation for published version (APA):
Jennings, S. J. A., Hambrey, M. J., & Glasser, N. F. (2014). Ice flow-unit influence on glacier structure, debris entrainment and transport. *Earth Surface Processes and Landforms*, *39*(10), 1279-1292. https://doi.org/10.1002/esp.3521

SPi	Journal Code				Article ID				Dispatch: 10.01.14	CE:
	E	S	P		3	5	2	1	No. of Pages: 14	ME:

EARTH SURFACE PROCESSES AND LANDFORMS
Earth Surf. Process. Landforms (2014)

Published online in Wiley Online Library
(wileyonlinelibrary.com) DOI: 10.1002/esp.3521

Ice flow-unit influence on glacier structure, debris entrainment and transport

Stephen J.A. Jennings,* Michael J. Hambrey and Neil F. Glasser
Centre for Glaciology, Department of Geography and Earth Sciences, Aberystwyth University, Aberystwyth, Ceredigion, SY23 3DB, UK

Received 2 July 2013; Revised 10 December 2013; Accepted 10 December 2013

*Correspondence to: Stephen J.A. Jennings, Centre for Glaciology, Department of Geography and Earth Sciences, Aberystwyth University, Aberystwyth, Ceredigion, SY23 3DB, UK. E-mail: saj7@aber.ac.uk

ESPL
Earth Surface Processes and Landforms

ABSTRACT: The links between structural glaciology, glacial debris entrainment and transport have been established in a number of different glacier settings. Here we document the structural evolution of a temperate Alpine valley glacier (Vadrec del Forno, Switzerland) and demonstrate that individual flow units within the glacier have very different structural and debris characteristics. The glacier consists of a broad accumulation area with multiple basins feeding a relatively narrow tongue and is formed from six distinct flow units. Each flow unit has its own characteristic structural assemblage. Flow units that narrow rapidly down-glacier are dominated by primary stratification that has evolved into longitudinal foliation. In contrast, wider flow units preferentially develop an axial planar foliation. Glacier structure plays a limited role in the entrainment of debris, which is more strongly influenced by ice-marginal rockfall and avalanche inputs onto the glacier surface. However, once entrained, glacier structure controls the reorientation and redistribution of debris within the ice mass. By taking a whole-glacier approach to describing glacier structure and debris transport, we conclude that individual flow units are unique with regard to structure and debris transfer. Copyright © 2013 John Wiley & Sons, Ltd.

KEYWORDS: Glacier structure; Debris entrainment and transport; Flow unit; Swiss Alps; Vadrec del Forno

Introduction

The aim of this paper is to investigate the structural evolution of a temperate Alpine valley glacier (Vadrec del Forno, Switzerland), and to demonstrate that individual glacier flow units exert a strong control on glacier structure and the entrainment and transport of debris. Many sediment–landform associations or landsystems preserve evidence of glacier structure, but on the whole the relationship with the source glaciers has only been defined in a few cases. Further work is important for reconstructing former glacier limits and thermal regime (Evans, 2003).

Recent research has focused primarily on the structural controls of debris transport in high-Arctic polythermal and cold-based glaciers. In particular, structural analysis of glacial sediments has been effectively applied to a number of valley glaciers in Svalbard (Bennett *et al.*, 1996; Hambrey *et al.*, 1996, 1999, 2005; Boulton *et al.*, 1999; Hambrey and Glasser, 2003b; Hubbard *et al.*, 2004). These studies have highlighted the importance of foliation, folding, and thrusting in controlling debris transport in polythermal and cold-based glaciers and how these processes constrain proglacial landform development. In contrast, there are comparatively few studies of temperate valley glaciers. Previous studies have commonly regarded debris transport as part of a larger scale glacial system (Drewry, 1972; Boulton and Eyles, 1979; Small, 1987; Kirkbride, 1995; Evans, 2003), or have focused only on the formation of certain debris-related glacial features (Boulton, 1967; Drewry, 1972; Eyles and Rogerson, 1978; Small *et al.*, 1979; Gomez and Small, 1985; Kirkbride and Spedding, 1996; Anderson, 2000). Nevertheless, a few studies have addressed structural controls on debris transport in contrasting temperate valley glaciers, notably Austerdalsbreen in Norway and the Berendon Glacier in the Canadian Rockies (Eyles and Rogerson, 1978), Haut Glacier d'Arolla in Switzerland (Goodsell *et al.*, 2005a, 2005b), Glacier de St. Sorlin in France (Roberson, 2008), and the lower Fox Glacier in New Zealand (Appleby *et al.*, 2010).

Vadrec del Forno differs from the previously studied temperate glaciers in having multiple accumulation basins that produce converging flow units, each mainly supplied with blocky granite clasts from precipitous head- and side-walls (Figure 1). Furthermore, years of negative mass balance have revealed ice-surface structures in remarkable detail. By applying structurally based sediment analysis techniques to this previously unstudied temperate valley glacier, we determine the ongoing structural evolution, debris-distribution processes, and dynamic history of the glacier, and thereby provide a basis for comparison with other Alpine valley glacier systems. F1

Study Area

Vadrec del Forno (46°17′N to 46°20′N, 9°40′E to 9°43′E) is a north-flowing temperate Alpine valley glacier, located in Val Forno near Passo del Maloja, southeast Switzerland. The glacier is approximately 5.3 km in length (Swiss Glacier Monitoring Network, 2013) and consists of a broad accumulation area that comprises two distinct basins feeding a relatively

Figure 1. View of the upper section of Vadrec del Forno from Capanna del Forno. Photograph taken August 2011.

narrow tongue, with a third joining the tongue halfway along its length (Figure 2). The two main accumulation basins have a maximum ice-surface altitude of *c.* 3200 m a.s.l., with the third tributary basin reaching an altitude of 2860 m a.s.l. The glacier snout terminated at 2240 m a.s.l in 2011. Between 1911 and 2011 the glacier receded 1.9 km, having advanced only for one season (1934–1935) since records began (Swiss Glacier Monitoring Network, 2013). The glacier terminates as a gently sloping convex snout, heavily pitted from both supraglacial and subglacial meltwater erosion. The immediate proglacial area is a braid-plain, flanked by uneven rubble slopes of basal and supraglacial debris. The bedrock geology of upper Val Forno and the mountains surrounding the glacier consist almost entirely of porphyritic granodiorite of Oligocene age (30 Ma), belonging to the Bregalia – Iorio Intrusive Complex that straddles the border of Switzerland and Italy (Trommsdorff and Connolly, 1996). The rocks are characterized by widely spaced joints, but there is no obvious structural feature controlling the location of the glacier.

Methods

Structural mapping

Satellite imagery interpretation

Satellite imagery and aerial photography has been regularly used for mapping glacier surface structures (Allen *et al.*, 1960; Meier, 1960; Hambrey and Milnes, 1977; Hambrey and Müller, 1978; Goodsell *et al.*, 2005a, 2005b; Hambrey *et al.*, 2005; Roberson, 2008; Appleby *et al.*, 2010). In the present study, the two-dimensional structure of Vadrec del Forno was established by tracing large-scale structural features from satellite imagery. Two sources of satellite imagery were used; higher resolution CNES/Spot imagery taken on 7 September 2010 sourced from Google Earth (Google Earth, 2013) and lower resolution imagery from summer 2005 sourced from the Switzerland Mobility website (Switzerland Mobility, 2013). Structural features were identified and mapped using the criteria outlined by Hambrey and Lawson (2000), Goodsell *et al.* (2005b), Cuffey and Paterson (2010), and verified in the field.

Field observations

Three-dimensional structures were identified in the field according to their dimensions, orientation, and cross-cutting relationships, using criteria outlined by Goodsell *et al.* (2005b). Structures identified on Vadrec del Forno included primary stratification, longitudinal foliation, axial planar foliation, folds, and various fracture systems. Three-dimensional measurements of structures were recorded using a compass/clinometer. The following attributes of each structure were recorded: length, shape, whether it was open or closed, evidence of displacement, debris content and size, ice-crystal size, ice colour, ice-crystal shape and alignment, and dip angle and dip orientation. From these data, the overall glacier structure and its sequential development were determined.

Sedimentary facies on the glacier surface

Samples of 50 clasts from 37 individual sediment facies were collected from a variety of locations on and around Vadrec del Forno (Figure 2), following the approach of Benn and Ballantyne (1994). The morphology of sediment features was recorded, including height, length, orientation, slope angle, and shape. Matrix descriptions including colour, degree of sorting, clast size-range, character of bedding, and the percentage of constituent grain sizes, were also documented. For each clast sampled the lithology, shape (following Hubbard and Glasser, 2005), roundness (following Powers, 1953), and texture (faceting, grooves, striations, and chipped edges), were recorded. Clast characteristics are recorded in RA/C_{40} scatterplots following Benn and Ballantyne (1994). Sedimentary facies derived from glacier ice are categorized according to the modification by Hambrey and Glasser (2003a) of Moncrieff's (1989) non-genetic classification of poorly sorted sediments.

Structural Composition of Vadrec del Forno

A range of planar structures and fractures were observed; these are organized sequentially from equilibrium line to snout using structural geological notation. Their attributes are given in

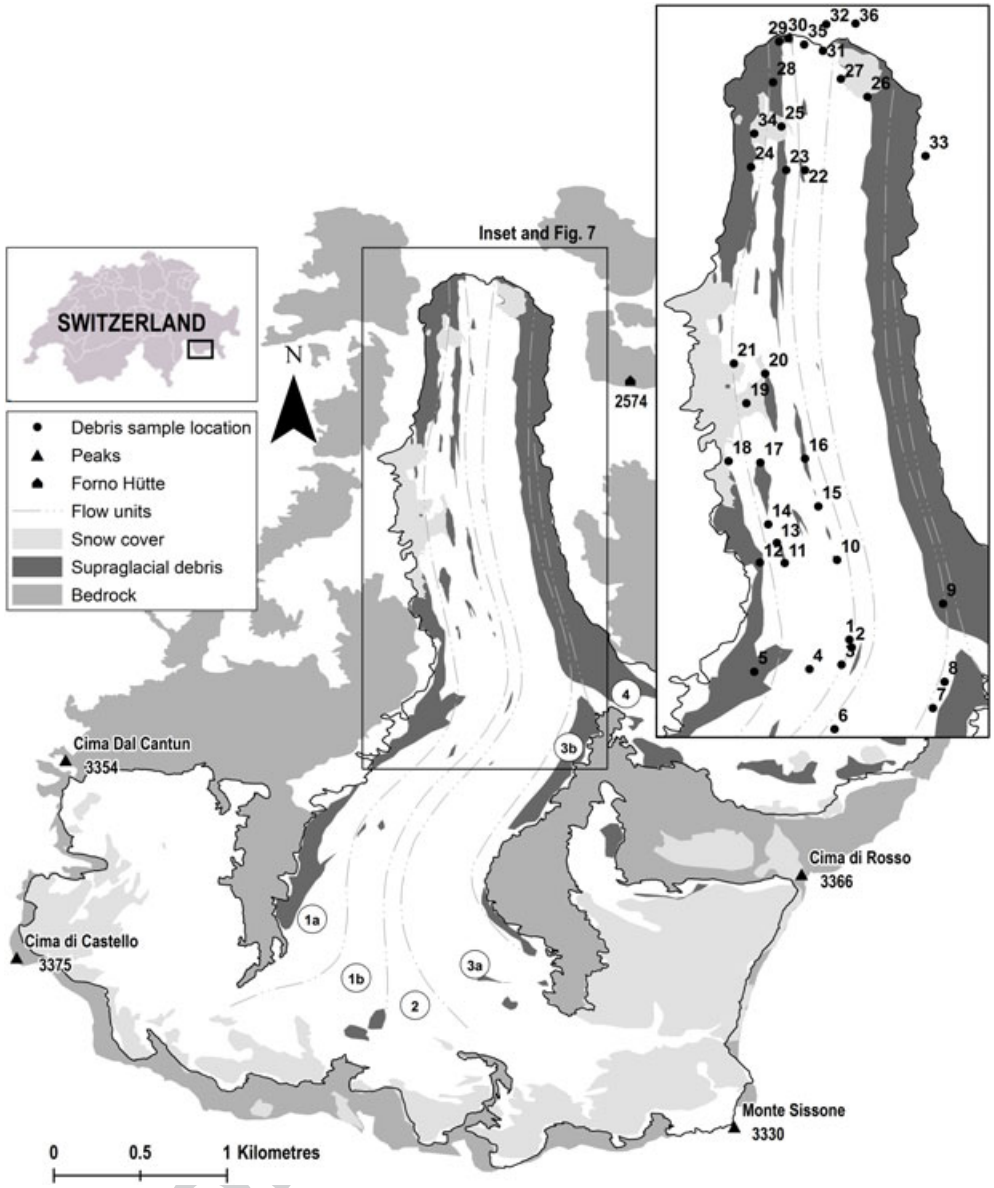

Figure 2. Flow unit map of Vadrec del Forno and location within Switzerland. Inset shows enlargement of glacier snout area and location of debris samples.

Table I along with their interpretation. These components are discussed in turn below.

Flow units

Vadrec del Forno is formed of six flow units, each of which can be traced back to its respective sub-accumulation basin (Figure 2). Flow units are characterized by relatively wide bands of arcuate planar structures (Figure 3). Prominent longitudinal anastomosing layers of coarse clear, coarse bubbly, and fine clear ice are found at flow-unit boundaries, becoming increasingly debris-rich down-glacier. This is especially true in the middle reaches of the glacier where medial moraines eventually form towards the snout. The central flow units can be traced directly from their respective sub-accumulation areas to the glacier snout; however, the lateral flow units become increasingly debris-covered and indistinct towards the terminus.

Arcuate planar structures (S_0)

Description

Irregular but continuous arcuate planar structures are observed primarily in the upper reaches of the glacier (Figure 3). Ice facies commonly consist of alternating layers of coarse bubbly, coarse clear, and fine bubbly ice, which tend to plunge gently up-glacier. Large-scale asymmetric folding occurs around flow-parallel fold axes with the strongest folding coinciding with flow-unit boundaries (Figure 4). Parasitic folds commonly occur on larger fold limbs. Structures present in the centre of flow units reflect the geometry of their individual sub-accumulation basins, becoming increasingly arcuate down-glacier.

Interpretation

Continuous arcuate planar structures are interpreted as primary stratification (S_0). The different ice facies reflect the layering of snow and firn preserved during firnification. Despite modification by melt and refreezing, the ice descriptions are consistent with previous interpretations of initial snowpack formation (Wadham and Nuttall, 2002). Low-density coarse bubbly ice, often observed in relatively thick layers, represents winter snow accumulation that has undergone partial melt and refreezing. High-density coarse clear ice represents the refreezing of meltwater and slush accumulation at the base of the snowpack. Generally thinner strata consisting of small (<5 mm) fine ice crystals represents summer snow accumulation.

Table I. Description and interpretation of structures, including sequential status and spatial distribution on Vadrec del Forno

Description	Interpretation	Notation	Location
Continuous layers initially parallel to equilibrium line; increasingly wavy down-glacier	Primary stratification	S_0	Ubiquitous in accumulation area
Attenuation of S_0 layering with fold axes parallel to inferred flow	Folding of stratification (S_0)	F_1	Ubiquitous
Anastomosing layers of coarse bubbly, coarse clear, and fine-grained ice; length of layers measured in metres, thickness a few centimetres	Longitudinal foliation	S_1	Well developed at flow-unit boundaries
As above but intersecting folded S_0	Axial planar foliation	S_1	Primarily found in flow unit 3a
Open fractures, up to a few metres wide. Continuous planar traces parallel to these and extending into them, comprising of coarse clear ice with crystals developed orthogonal to fracture margin and commonly showing a suture defined by bubbles in the middle	Transverse/ diagonal crevasses and crevasse traces	S_2	Ubiquitous
	Splaying crevasses and crevasse traces	S_3	Develops 100 metres from terminus
	Terminal arcuate crevasses and crevasse traces	S_4	Develops 20 metres from terminus

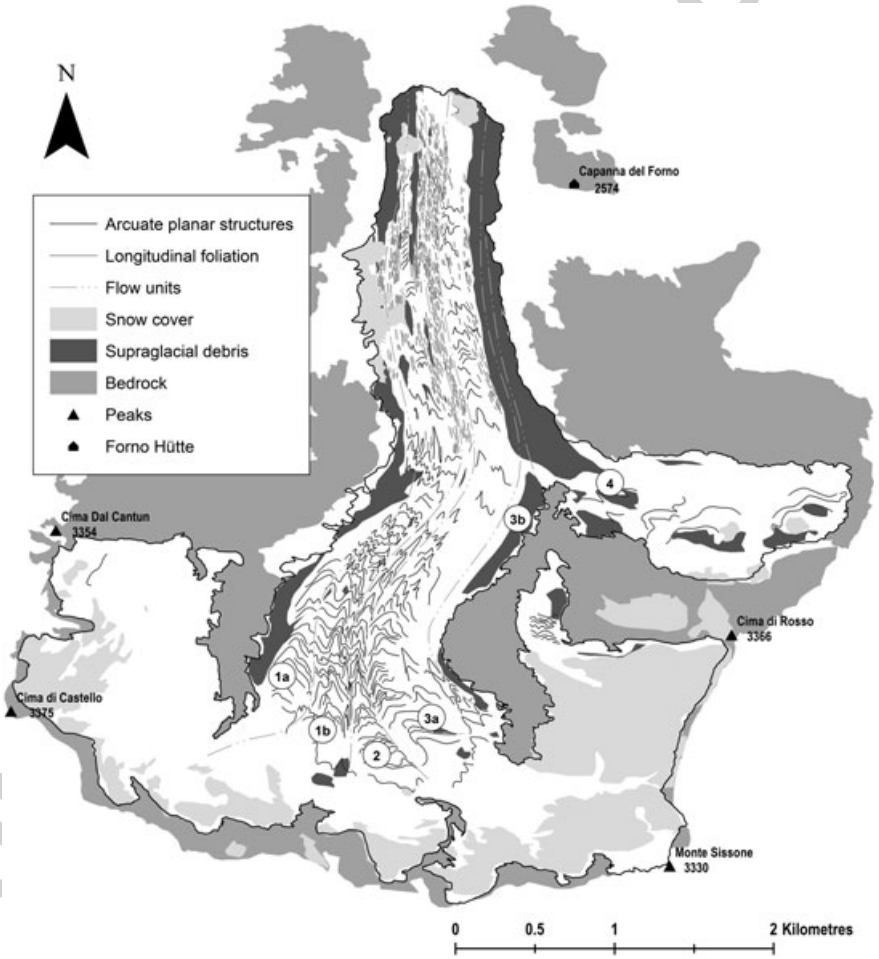

Figure 3. Structural map of ductile features, including arcuate planar structures (stratification) and longitudinal foliation.

Longitudinal planar structures (S_1)

Description

Steeply dipping longitudinal planar structures are evident across the majority of the glacier tongue (Figure 3). These structures are orientated parallel to and are most discernible at, flow-unit boundaries. Ice-facies composition is very similar to primary stratification (S_0), consisting of alternating layers of coarse clear, coarse bubbly, and fine-grained ice (Figure 4). Individual layers rarely exceed several tens of centimetres in thickness. Less frequent sub-centimetre-thick layers of fine white ice usually occur at flow unit boundaries.

Interpretation

Steeply dipping longitudinal planar structures are interpreted as longitudinal foliation (S_1). The similar ice facies composition of primary stratification (S_0) and longitudinal foliation (S_1) suggests that the latter represents a transition from the former. Longitudinal foliation evolves when transverse primary stratification becomes re-orientated by ductile flow. This occurs primarily in areas of converging flow which are dominated by simple shear regimes and longitudinal extension (Hambrey, 1977a; Hambrey and Lawson, 2000). However, fine white ice layers are not observed in primary stratification. Formation of these thin layers is most likely the result of crystallographic

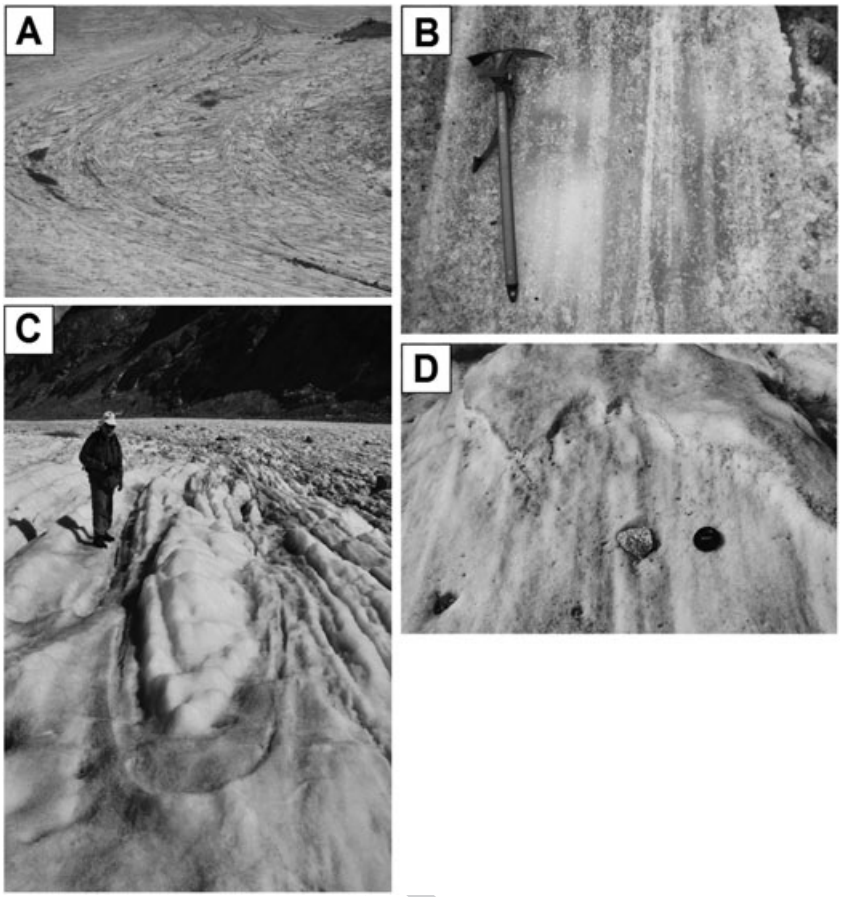

Figure 4. Ductile flow-related structures: (A) arcuate planar structures (folded primary stratification (S0)); (B) longitudinal foliation ice types; (C) isoclinal folding of primary stratification; (D) axial planar foliation; note the axial planar relationship with folded primary stratification.

modification of ice layers when experiencing simple shear. A second type of longitudinal planar structure was also observed in Vadrec del Forno. Axial-planar foliation cross-cuts primary stratification in a geometrically similar fashion to slaty cleavage seen in folded sedimentary rocks (Hambrey *et al.*, 2005). Unlike the formation of longitudinal foliation described above, axial-planar foliation is not derived from pre-existing structures. It is less common on the glacier than longitudinal foliation, yet forms preferentially where primary stratification is preserved relatively far down-glacier.

Fractures and continuous planar traces (S_2)

Description

Multiple sets of fractures are evident across the entire surface of the glacier (S_2) (Figures 5, 6, and 7). Continuous planar traces are common features in all flow units; however, open fractures are currently confined to the upper basins and lateral margins of the glacier. No open fractures exceeding 1 m in width were observed. Planar traces often extend for many tens of metres in length; however, no open crevasse exceeding *c.* 10 m was observed. Open fractures and planar traces cross-cut primary stratification and foliation development.

Interpretation

Open fractures and continuous planar traces are interpreted as crevasses and crevasse traces respectively. Open crevasses form either in the relatively steep accumulation basins in response to extending flow (Figure 6), or on the glacier's flanks resulting from shear stresses at the lateral margins. Fractures resulting from extending flow develop normal to the principal tensile stress tensor, producing linear traces transverse to flow which become increasingly convex down-glacier over time. Fractures on the lateral margins of the glacier configure themselves as chevron crevasses, which are linear fractures aligned obliquely up-glacier (Benn and Evans, 2010). Two main processes lead to crevasse trace genesis: (i) refreezing of meltwater in open crevasses; (ii) propagation of tensional veins whereby new ice crystals grow parallel to the principal tensile stress tensor (Hambrey *et al.*, 2005). The majority of crevasse traces appear in the upper reaches of the glacier, within or close to areas of open fractures. This along with the presence of so many crevasse traces in comparison with open crevasses suggests that crevasse traces primarily form as tensional veins, either as fractures in their own right, or as continuations of open crevasses. The presence of crevasse traces near the glacier snout, despite undergoing substantial ablation, suggests that fracture propagation must be relatively deep, possibly reaching the bed. This phenomenon has been noted on other valley glaciers (Hambrey and Müller, 1978). Additionally the cross-cutting relationship between crevasse traces and other structures highlights the fact that fracture formation succeeds primary stratification and foliation development.

Longitudinal fractures (S_3)

Description

Longitudinal fracture sets comprising open vertical fractures extending up to 50 m in length and no greater than 1 m in width are found exclusively at the glacier snout.

Interpretation

Longitudinal fractures are interpreted as splaying crevasses (S_3). As the tongue narrows as a result of ablation, the lateral margins

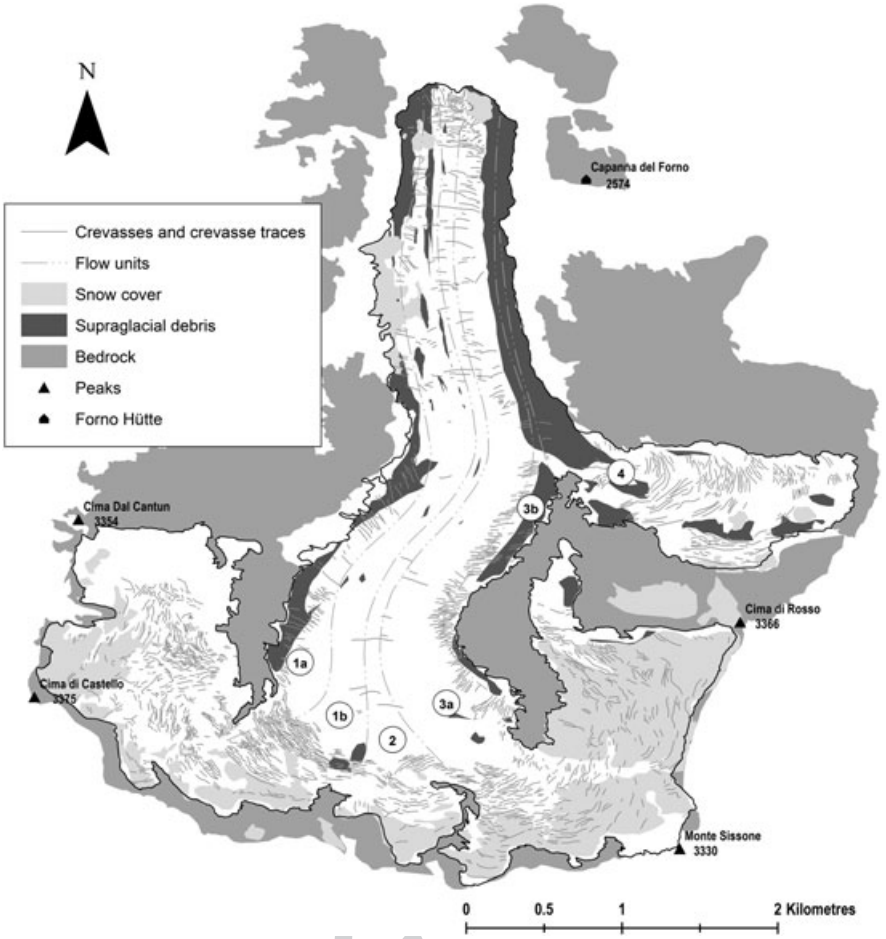

Figure 5. Structural map of brittle features: crevasses and crevasse traces.

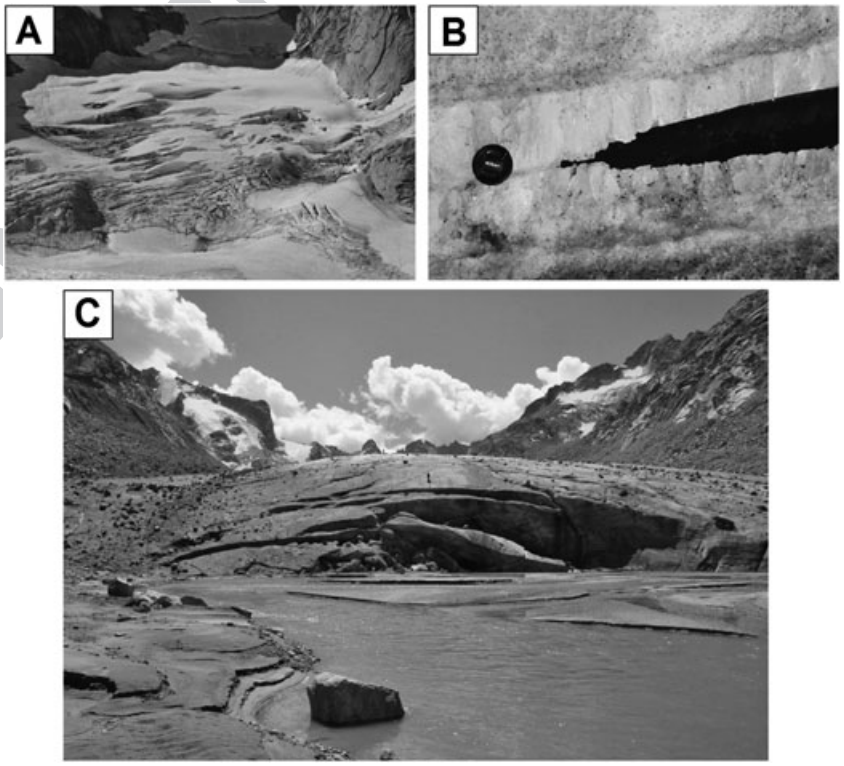

Figure 6. Brittle fracture related structures: (A) open crevasses in the upper accumulation area as a result of extending flow; (B) a partially healed, water-filled crevasse; note the ice crystals growing perpendicular to the crevasses edge; (C) open arcuate crevasses on the true right of the glacier. It is suspected that the enlargement of an abandoned subglacial cavity is responsible for crevasse formation.

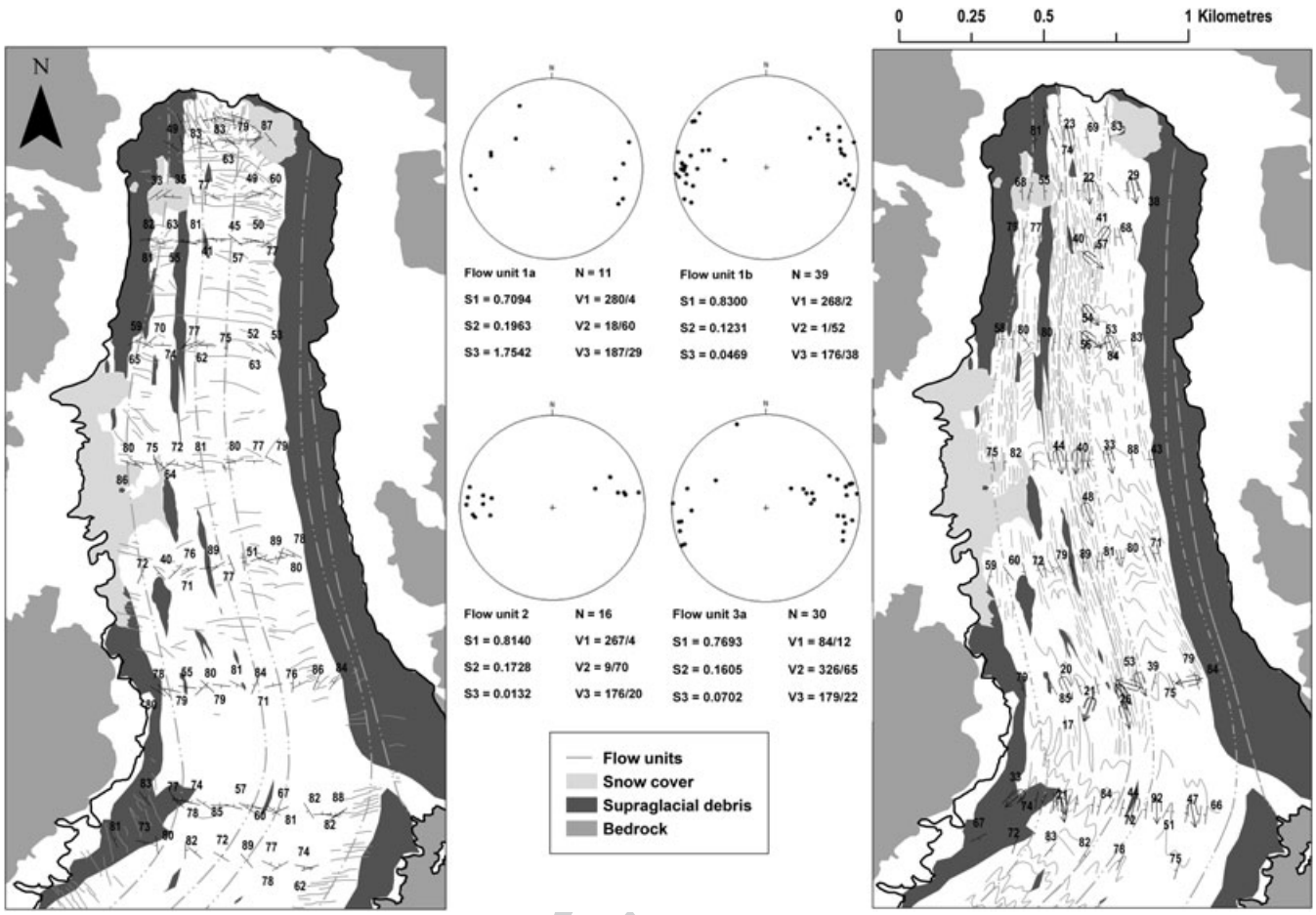

Figure 7. Left: structural measurements of crevasse and crevasse trace dip-angle and orientation. Right: structural measurements of primary stratification and longitudinal foliation dip angle and orientation. Centre: Schmidt lower-hemisphere equal area projection of poles to foliation with eigenvalues and eigenvectors shown alongside.

of the glacier no longer abut against the lateral moraines. Subsequently at the glacier's snout some extension transverse to glacier flow can occur where the glacier is no longer confined by its lateral moraines, allowing longitudinal fractures to open parallel to the main glacier flow direction.

Arcuate fractures (S_4)

Description

On the true-right of the glacier are a series of arcuate fractures orientated concave down-glacier. The fractures are *c.* 100 m in length and range from 0.5 to 2 m in width. They are situated behind a small ice cliff on the snout of the glacier (Figure 6).

Interpretation

Arcuate fractures are interpreted as crevasses which have opened as a result of the enlargement of a subglacial cavity (S_4). Fracturing usually occurs on the lateral margins of a glacier as a result of shear stresses, or in zones of extending flow. As neither process is active in the vicinity of the arcuate fractures, and the area is unaffected by valley morphology, the enlargement of a subglacial cavity is inferred. This process, which is increasingly common on alpine glaciers as recession and, increasingly stagnation, leads to a reduction in internal deformation that would otherwise result in cavity closure. At the time of the field study, subglacial meltwater preferentially emerged from the terminus on the true-left of the glacier. This suggests that the cavity on the true-right of the glacier was once a subglacial conduit, and that it was subsequently abandoned.

Circular/elliptical void structures

Description

A variety of circular/elliptical void structures were observed at Vadrec del Forno. Their size varies, ranging from a few tens of centimetres in length through to *c.* 4 m. Two types of void were observed; fully healed, and water-filled. Healed structures rarely exceed *c.* 1 m in length, consisting of blue ice crystals *c.* 10–15 cms long, growing perpendicular to the structure's edge. All other void structures were water-filled.

Interpretation

Circular/elliptical crystal structures are interpreted as crystal quirks, following Stenborg (1968). Their formation represents the recrystallization of voids originally existing as moulins or englacial drainage features (Goodsell *et al.*, 2005b).

Sedimentary Facies at the Ice Surface

Three ice-surface sedimentary facies were observed on Vadrec del Forno: angular gravel, subangular gravel, and gravelly muddy sand. Differentiation between sedimentary facies was achieved using clast roundness, clast-surface texture, particle-size distributions, degrees of sorting, and RA/C_{40} indices (Table II and Figure 8). A fourth facies of little volumetric significance, but nevertheless forming prominent mounds, comprises silt nodules.

Table II. Sedimentary facies categorized according to the modification by Hambrey and Glasser (2003a) of Moncrieff's (1989) non-genetic classification of poorly sorted sediments

Lithofacies	Subfacies	Sample sites	Sorting	Percentage			Clast roundness	Structural association
				g	s	m		
Gravel	Angular gravel	1, 2, 3, 6, 7, 8, 9, 10, 11, 13, 14, 15, 16, 17, 20, 24, 25, 27, 34	Very poorly sorted	80	15	5	VA, A	Medial moraines. Supraglacial debris parallel to longitudinal foliation (S_1)
Gravel	Subangular gravel	5, 18, 19, 23, 28, 29, 30, 33	Poorly sorted	70	20	10	A, SA	Reworked medial and lateral moraine debris
Sand	Gravelly muddy sand	4, 12, 21, 26, 31, 32, 36, 37	Moderately well sorted	15	60	25	SA, SR	Glaciofluvial and debris cones
Mud	Mud	-	Very well sorted	0	0	100	-	Silt nodules associated with crystal quirk sediment traps

Angular gravel

Description

The angular gravel facies represents the most volumetrically abundant supraglacial sediment type. Primarily associated with medial and lateral moraines, it is characterized by poorly sorted debris with a wide clast-size distribution. RA values are high (*c.* 70–100%) with moderate C_{40} values (*c.* 20–60%) (Figure 8). Angular gravel predominantly appears as flow-parallel lenticular ice-cored debris mounds in the upper reaches of the glacier, eventually forming medial moraines lower down the glacier. This facies is dominated by the gravel fraction (typically cobbles and boulders), often exceeding 80% by volume. The remaining fractions consist primarily of coarse (1–2 mm) angular sand with some silt. Isolated granodiorite boulders on the surface attain several metres in length (a-axis) (Figure 9). **F9**

Interpretation

The angular properties and supraglacial distribution indicate that the angular gravel facies is rockfall debris that has been concentrated at flow-unit boundaries. Rockfall from the walls of the upper basin becomes entrained in primary stratification (S_0) during firnification. Subsequent folding (F_1) of primary stratification concentrates entrained debris at flow-unit boundaries. Surface ablation reveals the septa between flow units eventually forming medial moraines (Figure 9).

Subangular gravel

Description

The second most volumetrically abundant sedimentary facies is subangular gravel (Figure 9). Like the angular gravel facies, subangular gravel is primarily associated with lateral and medial moraines. However, this facies also includes samples collected from some englacial debris layers. Subangular gravel is characterized by poorly sorted debris with a wide clast-size distribution. The gravel fraction is dominant, usually exceeding 80% by volume. The remaining fractions comprise mainly sand with some silt. RA values are moderate (*c.* 20–60%) with relatively low C_{40} values (*c.* 10–40%) (Figure 8).

Interpretation

The similar characteristics of angular and subangular gravel facies suggest that they share a common process of formation. However, some clasts in the subangular gravel facies have undergone a greater degree of edge-rounding. Rockfall debris becomes entrained in primary stratification (S_0) and deforms during the folding phase (F_1). During deformation, or subsequent to supraglacial re-emersion, the angular clasts undergo a phase of edge-rounding as clasts collide and abrade against one another, producing the subangular gravel. A sandy gravelly mud facies found in avalanche deposits are broadly similar to the rockfall-derived facies. Avalanche deposits are also poorly sorted. However, the gravel fraction was respectively low (*c.* 30% by volume); the mud fraction was dominant (*c.* 50%), with the sand fraction also achieving a relatively high percentage (*c.* 20%). Despite sharing a similar source material to rockfall debris, avalanche deposits are subject to a greater degree of modification. Snow avalanches, also referred to as 'snowflows', are viscous flows of material that transports debris by a combination of turbulent suspension and bedload traction (Blikra and Nemec, 1998). The resulting fracturing and abrasion of clasts against one another, combined with the mixing of debris, snow, and meltwater, preferentially forms finer sediment fractions.

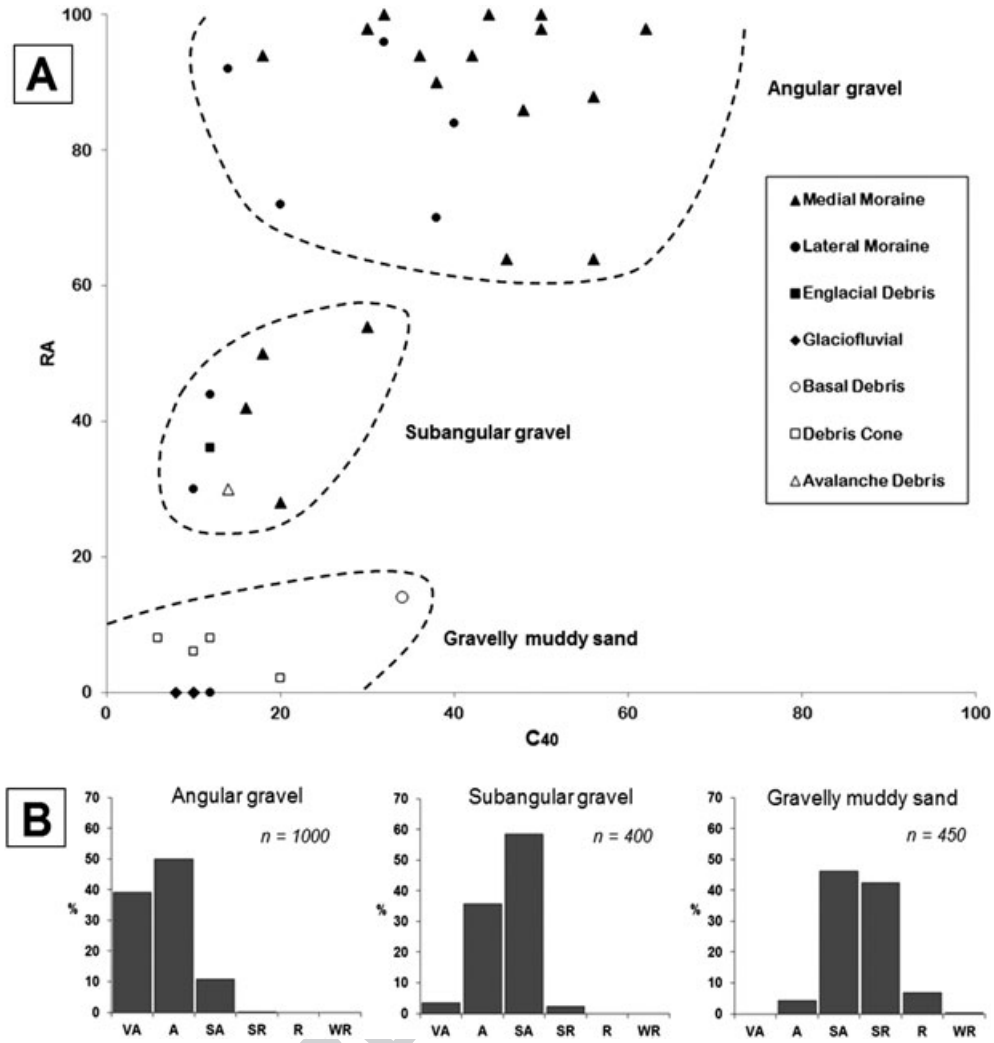

Figure 8. (A) RA/C40 scatterplot of clast characteristics; (B) Powers roundness histograms for ice-surface sediment facies.

Gravelly muddy sand

Description

The least volumetrically abundant sediment facies found on the glacier is gravelly muddy sand (Figure 9). This sediment facies was observed only on the glacier margins, and is much more common in the proglacial zone. The sediment is generally well-sorted and contains clast sizes ranging from silt to small cobbles. The sand fraction commonly dominates the sediment facies (*c.* 35–80%), with mud (*c.* 10–50%) and gravel (*c.* 10–30%) in lesser abundance. RA values are low (*c.* 0–15%) with low to moderate C_{40} values (*c.* 0–40%) (Figure 8). Two suites of ice-cored debris cones located on opposite sides of the glacier comprised the majority of supraglacial gravelly muddy sand deposits (Figure 9): (i) debris cones on the true left of the glacier were located next to an open crevasse which had a *c.* 1–2 cm thick layer of sediment-rich ice frozen around the structure's edge. The debris cover of the cones contained sub-millimetre sedimentary stratification. (ii) Debris cones on the true right of the glacier were located next to an abandoned sediment-clogged moulin system. No sedimentary stratification was observed for this suite of debris cones.

Interpretation

The rounded clasts and moderately well-sorted nature of the gravelly muddy sand deposits suggest a glaciofluvial origin. This is further supported by the dominance of the sediment facies in the proglacial zone. The high sand fraction combined with low RA values is indicative of a relatively high-energy fluvial environment, such as the subglacial hydrological system. A well-developed subglacial hydrological system explains the lack of entrained subglacial sediments. High basal melt-rates remove debris that became entrained in the basal ice. Some limited gravelly muddy sand debris was observed at the snout of the glacier, resulting from localized re-entrainment of subglacial sediments. Supraglacial gravelly muddy sand deposits were primarily observed in a number of ice-cored debris cones located on the glacier's margins (Figure 9). Ice-cored debris cones form as a result of debris cover insulating the underlying ice. Differential ablation results in the more rapid lowering of the surround ice surface, producing an ice mound (Drewry, 1972). However, a number of different processes may provide a source for the debris cover. Debris cones are often derived from fine sediments washed out of lateral and medial moraines which become concentrated in supraglacial streams. Thickening of sediment in abandoned pools, bars, or moulins is commonly sufficient to insulate the underlying ice (Drewry, 1972). However, other mechanisms include thrusting of subglacial sediments to form debris-charged ridges at the glacier surface (Jansson *et al.*, 2000; Glasser *et al.*, 2003), concentrations of aeolian-derived dust and volcanic tephra (Krenek, 1958), and rockfall debris. Two different origins for the suites of debris cones on opposite sides of Vadrec del Forno are suggested.

(i) Debris cones on the true left of the glacier appear to have had basal sediments injected onto the ice surface via an open crevasse. This was inferred from observations of the

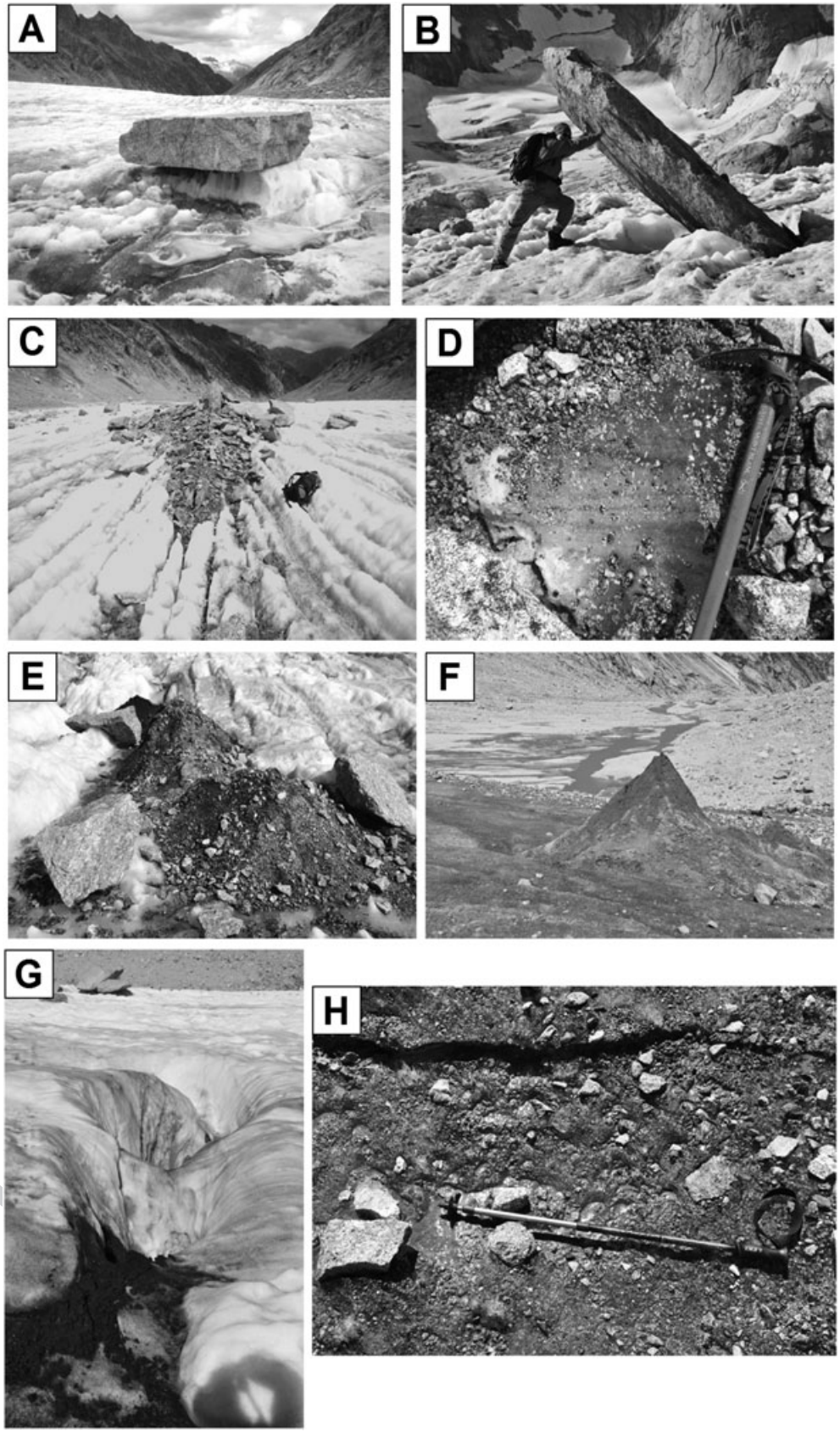

Figure 9. Sedimentary facies, dominated by granodiorite clasts: (A) large solitary angular block; (B) subangular block emerging parallel to primary stratification (S0); (C) the emergence of a medial moraine; (D) subangular gravel (note the foliated ice running horizontally across the picture); (E) gravelly muddy sand; (F) debris cone of gravelly muddy sand on the true right of the glacier; (G) relatively large build-up of dark silt in an abandoned supraglacial stream; (H) basal ice debris found in the snout of the glacier.

supraglacial debris cover originating from an open crevasse which had a layer of sediment-rich ice frozen around its edge. High basal water pressures and a crevasse which propagates to the bed would be required. 'Spring events' have been documented for other Alpine glaciers (Mair *et al.*, 2003). Rapid inputs of meltwater are introduced to a poorly developed subglacial hydrological system after the winter season. Subsequent high basal water pressures

can decouple the glacier from its bed, resulting in an increase in flow velocity (Mair *et al.*, 2003). Increases in basal water pressure at the glacier margins may have been sufficiently high to inject sediment-rich water on to the ice surface.

(ii) Debris cones on the true right of the glacier are located next to an abandoned sediment-clogged moulin system. The moulin-fill forms a substantial englacial debris package. Surface ablation reveals the moulin-fill as supraglacial debris cover, protecting the underlying ice from further ablation, resulting in the formation of an ice-cored debris cone.

Silt nodules

Black balls of silt are of limited extent on the surface of the glacier (Figure 9). These nodules comprise relatively fine sediments (<1 mm) and rarely exceed *c.* 10 cm in width. Silt deposits are commonly found near active and abandoned supraglacial streams, and tended to have reasonably high moisture contents. The silt is thought to originate from aeolian-derived dust and organic material, which has become trapped in surface ice (Oerlemans *et al.*, 2009). Surface ablation entrains trapped fines into supraglacial streams where the silt fraction is deposited in stagnant pools.

Discussion

Glacier-wide systems

A glacier-wide approach is required to fully understand the structural impacts of an ice mass upon debris distribution. Smaller-scale structure-debris relationships can be observed in all ice masses to varying degrees; however, larger-scale variables give individual glaciers their unique characteristics.

Adequately describing a glacial system can be problematic as larger-scale systems tend to be over-generalized. To overcome this, the ice mass must be separated into a number of smaller constituent parts. Previous studies have attempted to separate the glacier system into different longitudinal stress regimes, e.g. extending and compressing flow (Nye, 1952; Allen *et al.*, 1960). This study suggests a different approach, adopting flow units as the basic components of a glacier system. Flow units originate from their own individual sub-accumulation basins. Each basin has unique characteristics, which will be reflected in its corresponding flow unit.

Transverse and longitudinal stress regimes play an important role in the formation of brittle structures in ice masses, especially crevasses and crevasse traces (Hambrey and Müller, 1978; Harper *et al.*, 1998; Nath and Vaughan, 2003). Stress regimes vary greatly across the length and breadth of a glacier (Harper *et al.*, 1998). Stress also varies within flow units. Ductile structures, such as foliation and folding reflect cumulative strain, acquired as a 'parcel' of ice passing through different stress regimes. These structures may reflect either simple shear (e.g. longitudinal foliation), or pure shear (e.g. transverse foliation, as on other glaciers) (Hambrey and Milnes, 1977; Hooke and Hudleston, 1978; Hambrey and Lawson, 2000), depending on the location of the 'parcel' of ice within a flow unit. However, a flow unit broadly experiences uniform extending and compressing flow when compared with the whole-glacier-system. It is further inferred that ice velocities of individual flow units on the Vadrec del Forno vary. Differences in the dip angles of structures suggest that there are velocity variations between flow units (Figure 7). Therefore, by describing the ice dynamics for a number of parallel flow unit systems within an ice mass, the differences in extending and compressing flow across the glacier can be deduced.

Interactions between flow units on Vadrec del Forno are considered to be relatively unimportant with regard to structure-sediment relationships. Flow-unit inputs vary as a result of the unique characteristics of their corresponding sub-accumulation basins. Throughputs such as ice velocity and stress regimes also differ between flow units. Consequently, each flow unit has its own characteristic structural assemblage. This can be seen on Vadrec del Forno where unique flow evolutions have preferentially formed longitudinal and axial planar foliation in flow units 2 and 3a, respectively. Debris inputs into separate flow units also generally remain within their corresponding system. Simple shear at flow unit boundaries concentrates debris into septa; however, very little debris is interchanged between flow units. This suggests that medial moraines are not a product of inter-flow unit relationships; they are a result of separate flow unit processes simultaneously occurring at a mutual boundary between neighbouring systems.

Flow unit differences

Although Vadrec del Forno is a relatively small ice mass, it has a suite of structures at least as complex as many larger ice masses (Table III). The six constituent flow units of the glacier are inherently different from one another, and this is reflected in the different sedimentological attributes. T3

Despite the differences between flow units, each of the constituent parts of Vadrec del Forno are structurally dominated by the evolution of primary stratification (S_0) into longitudinal or axial planar foliation (S_1), accompanied by folding (F_1) with axial planes parallel to foliation. Longitudinal and axial planar foliations have different origins. Longitudinal foliation (S_1) is inherited from primary stratification (S_0) as it becomes folded (F_1). Continuing deformation in pure and simple shear regimes attenuates the limbs of the folds, eventually transposing primary

Table III. A comparative table of structures on other Alpine glaciers

	Vadrec del Forno	Bas Glacier d'Arolla	Haut Glacier d'Arolla	Glaceir de St. Sorlin	Griesgletscher
Number of flow units	6	1 (lower)	2	6	2
Primary stratification	✓	✓	✓	✓	✓
First fold phase	✓	✓	✓	✓	✓
Longitudinal foliation	✓	-	✓	✓	✓
Crevasses / traces 1	✓	✓	✓	✓	✓
Second fold phase	-	✓	-	-	✓
Transverse foliation	-	✓	-	-	✓
Thrusts	-	-	✓	✓	-
Ogives	-	✓	-	-	-
Source	This paper	Goodsell *et al.*, 2002	Goodsell *et al.*, 2005a	Roberson, 2008	Hambrey and Milnes, 1977

stratification (S_0) into longitudinal foliation (S_1); a similar process as observed in metamorphic rocks (Hobbs *et al.*, 1976; Hambrey and Lawson, 2000). Often, the only visible evidence of the original primary stratification once transposed is isolated remnant fold hinges (Hambrey, 1977a). Axial planar foliation on the other hand does not evolve from pre-existing structures. Foliation as a new structure has been observed in this study, as well as in surge-type temperate glaciers (Lawson *et al.*, 1994), temperate Alpine valley glaciers (Goodsell *et al.*, 2005b), and polythermal glaciers (Hambrey *et al.*, 1999, 2005). In a similar manner to longitudinal foliation, axial planar foliation is often longitudinally orientated. However, unlike longitudinal foliation, axial planar foliation has a clear axial planar relationship with primary stratification (S_0), cross-cutting the stratification (Figure 4). Superficially, this resembles the folding/slaty cleavage relationship found in low-grade metamorphic rocks such as mudstones. However, the exact mechanism of formation is unknown (Hambrey and Lawson, 2000). Differences in the dominance of longitudinal or axial planar foliation between flow units on Vadrec del Forno suggests that the primary type of foliation formed is location-dependent. The dominant force associated with longitudinal foliation development is strong lateral compression where flow converges and simple shear occurs at flow-unit boundaries (Hambrey and Lawson, 2000; Hambrey and Glasser, 2003b; Goodsell *et al.*, 2005b). This suggests that lateral compression and simple shear regimes differ between flow units at least in the convergence zone. Comparison of flow-unit widths down-glacier highlights differences in the amount of lateral compression (Figure 10). Flow unit 2 in particular narrows rapidly down-glacier, whereas flow unit 3a has less pronounced narrowing. Higher rates of simple shear are inferred in those flow units that have the most pronounced rate of lateral narrowing (e.g. flow unit 2). As a result, primary stratification (S_0) is quickly transposed into longitudinal foliation (S_1) in these flow regimes. This effect is further exacerbated by pure shear experienced in the centre of the flow unit. Conservation of mass dictates that when an object undergoes lateral compression, longitudinal or vertical extension must result to preserve its volume (volume change as a result of melt is considered to be comparatively negligible). Increased longitudinal extension aids attenuation of primary stratification (S_0) as it transposes into longitudinal foliation (S_1), increasing the rate of formation. In flow units that experience less pronounced narrowing (e.g. flow unit 3a), cumulative strain values are inferred to be lower allowing primary stratification to be preserved further down-glacier. Axial planar foliation tends to dominate these flow units. This suggests that high cumulative strain values and the rapid formation of longitudinal foliation destroy any evidence of axial planar foliation. Thus on Vadrec del Forno axial planar foliation is observed only in flow unit 3a.

Structural controls on debris entrainment and transfer

Glacier structure has limited control over debris entrainment in Vadrec del Forno, in marked contrast to other glaciers, especially those of polythermal regime in Svalbard (e.g. Midtre Lovénbreen, Finsterwalderbreen, Bakaninbreen, Kongsvegen; *cf.* Hambrey *et al.*, 1999). Entrainment by open crevasses is comparatively rare, involving insignificant amounts of debris. High basal melt rates further restrict subglacial entrainment processes (Glasser and Hambrey, 2002). The main input of debris into Vadrec del Forno is controlled by the spatial distribution of rockfall debris in the upper basins of the glacier. Rockfall occurrence is primarily determined by the character of the granodiorite bedrock. Rockfall events are spatially non-uniform, despite the relatively homogeneous nature of the bedrock. It is, therefore, likely that freeze–thaw processes acting on joint systems are the origin of many rockfall events, dictating the spatial distribution of debris input into the glacier.

The strongest structure-debris association is with primary stratification and subsequent folding. Debris is entrained within the snow-pack and progressively buried forming discontinuous structural layers within the ice mass. Once the debris package is confined within the structure of the glacier, the adjacent ice and debris strata remain parallel despite modification by ductile folding (F_1), suggesting that sediment redistribution and reorientation within a glacier is primarily controlled by glaciological structure.

Once debris re-emerges on the surface of the glacier as a result of ablation, other ice structures can cause limited re-entrainment of debris. Opening of chevron crevasses at the lateral margins of the glacier results in englacial re-entrainment of debris by filling of crevasses. Structurally controlled supraglacial fluvial processes also lead to re-entrainment of debris. Supraglacial drainage channels preferentially form in areas of

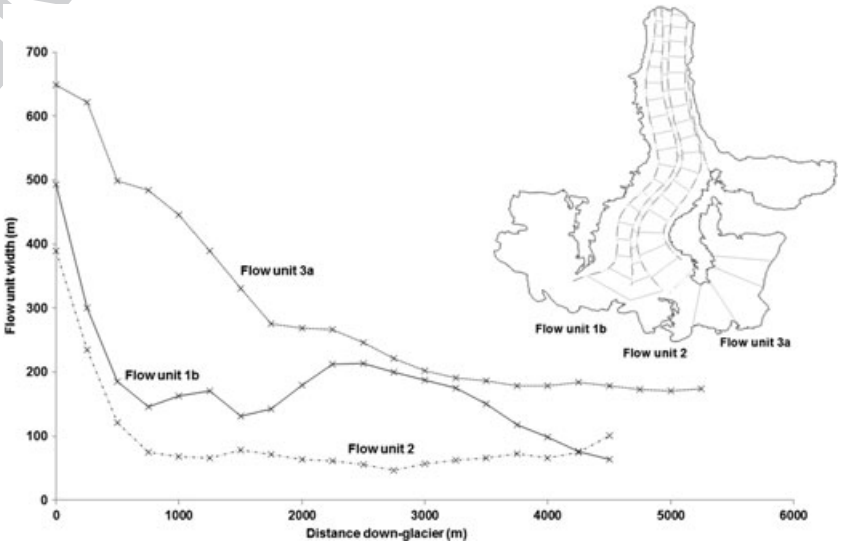

Figure 10. Variations in width measurements for flow units 1b, 2, and 3a. Inset: overview map of Vadrec del Forno with the location of width measurements taken.

steeply dipping longitudinal foliation (S_1), as do moulins which often form at the intersection of a crevasse trace (Stenborg, 1968; Hambrey, 1977b). Medial moraines also emerge in areas of steeply dipping longitudinal foliation (Hambrey and Glasser, 2003b; Goodsell *et al.*, 2005b), supplying debris to supraglacial streams. Only relatively small debris particles (<4 mm in diameter) can be re-entrained in this way because of the minimal entrainment capability of small supraglacial streams. However, limited entrainment of larger clasts can be achieved by moulin expansion, since the maximum size of clasts that are able to be entrained by moulin expansion is dependent upon the size of the moulin. However, clasts with an a-axis length of up to 50 cm were observed being entrained in this manner on Vadrec del Forno.

Conclusions

The investigation of the structure of Vadrec del Forno and debris-entrainment characteristics has yielded a number of similarities with, and differences from, other valley glaciers. By focusing on how multiple flow units interact, this paper adds to our understanding of debris-entrainment and transport processes in temperate valley glaciers.

The structure of Vadrec del Forno is dominated by the evolution of primary stratification (S_0) into longitudinal or axial planar foliation (S_1). Structural differences between flow units suggest that the formation of foliation is location-dependent. Comparison of flow-unit widths down-glacier indicate that longitudinal foliation-dominated flow units experience greater cumulative shear strain. Flow units that experience less cumulative shear strain preserve primary stratification (S_0), enabling axial-planar foliation to develop. Glacier structure plays a limited role in the entrainment of debris at Vadrec del Forno, unlike at other, especially polythermal, glaciers. Lithological variables determine the location and amount of debris-input to the glacier. Primary stratification (S_0) encloses supraglacial debris, entraining it into englacial positions. Once entrained, primary stratification (S_0) dictates how debris is redistributed and reorientated within the ice mass, through folding (F_1), especially at flow-unit boundaries. Englacial debris layers remain parallel to primary stratification (S_0). Transposition of primary stratification (S_0) to longitudinal foliation (S_1) occurs under simple shear at flow unit boundaries. Englacial debris becomes concentrated and orientated parallel to steeply dipping longitudinal foliation. Ice ablation reveals septa between flow units as medial moraines. Glacier structure controls re-entrainment of supraglacial debris at flow-unit boundaries. Medial moraines, supraglacial streams, and moulins preferentially form in areas of near-vertical longitudinal foliation. Fluvial reworking of gravels entrains fine particles. Transported debris in supraglacial streams is re-entrained by moulins. Some larger clasts can be englacially re-entrained by moulin expansion.

Flow units originate in their own individual sub-accumulation basins, and thus reflect the attributes and inputs in their corresponding basins. Characteristics such as basin size, altitude and snow input determine the dominance of the flow unit within the whole-glacier system. Individual flow units are unique with regard to structure and debris transfer.

Acknowledgements—SJAJ would like to thank Natalie Davies for her assistance with fieldwork and data processing. Mary and Arthur Jennings are greatly thanked for their financial and moral support. The Centre for Glaciology, Aberystwyth University, supplied field equipment. MJH thanks Dr Jürg Alean for support in the field. The constructive comments of two anonymous reviewers are gratefully acknowledged.

References

Allen CR, Kamb WB, Meier MF, Sharp RP. 1960. Structure of the lower Blue Glacier, Washington. *Journal of Geology* **68**(6): 601–625.

Anderson RS. 2000. A model of ablation-dominated medial moraines and the generation of debris-mantled glacier snouts. *Journal of Glaciology* **46**(154): 459–469.

Appleby JR, Brook MS, Vale SS, MacDonald-Creevey AM. 2010. Structural glaciology of a temperate maritime glacier: Lower Fox Glacier, New Zealand. *Geografiska Annaler* **92**(A): 451–467.

Benn DI, Ballantyne CK. 1994. Reconstructing the transport history of glacigenic sediments: a new approach based on the covariance of clast shape indices. *Sedimentary Geology* **91**: 215–227.

Benn DI, Evans, DJA. 2010. *Glaciers and Glaciation*. Hodder Education: London.

Bennett MR, Hambrey MJ, Huddart D, Ghienne JF. 1996. The formation of geometrical ridge networks ('crevasses-fill' ridges), Kongsvegen, Svalbard. *Journal of Quaternary Science* **11**: 430–438.

Blikra LH, Nemec W. 1998. Postglacial colluvium in western Norway: depositional processes, facies and palaeoclimatic record. *Sedimentology* **45**: 909–959.

Boulton GS. 1967. The development of a complex supraglacial moraine at the margin of Sorbreen, Ny Friesland, Vestspitzbergen. *Journal of Glaciology* **6**: 717–736.

Boulton GS, Eyles N. 1979. Sedimentation by valley glaciers: a model and genetic classification. In *Moraines and Varves*, Schluchter C (ed). Balkema: Rotterdam.

Boulton GS, van der Meer JJM, Beets DJ, Hart JK, Ruegg GHJ. 1999. The sedimentary and structural evolution of a recent push moraine complex: Holmstrombreen, Spitsbergen. *Quaternary Science Reviews* **18**(3): 339–371.

Cuffey KM, Paterson WSB. 2010. *The Physics of Glaciers*. Elsevier: Oxford.

Drewry DJ. 1972. A quantitative assessment of dirt-cone dynamics. *Journal of Glaciology* **11**(63): 431–446.

Evans DJA. 2003. *Glacial Landsystems*. Arnold: London.

Eyles N, Rogerson RJ. 1978. A framework for the investigation of medial moraine formation: Austerdalsbreen, Norway and Berendon Glacier, British Columbia, Canada. *Journal of Glaciology* **20**: 99–113.

Glasser NF, Hambrey MJ. 2002. Sedimentary facies and landform genesis at a temperate outlet glacier: Soler Glacier, North Patagonian Icefield. *Sedimentology* **49**: 43–64.

Glasser NF, Hambrey MJ, Etienne JL, Jansson P, Pettersson R. 2003. The origin and significance of debris-charged ridges at the surface of Storglaaciären, northern Sweeden. *Geografiska Annaler* **85A**: 127–147.

Gomez B, Small RJ. 1985. Medial moraines of the Haut Glacier d'Arolla, Valais, Switzerland: debris supply and implications for moraine formation. *Journal of Glaciology* **31**(109): 303–307.

Goodsell B, Hambrey MJ, Glasser NF. 2002. Formation of band ogives and associated structures at Bas Glacier d'Arolla, Valais, Switzerland. *Journal of Glaciology* **48**(161): 287–300.

Goodsell B, Hambrey MJ, Glasser NF. 2005a. Debris transport in a temperate valley glacier: Haut Glacier d'Arolla, Valais, Switzerland. *Journal of Glaciology* **51**(172): 139–146.

Goodsell B, Hambrey MJ, Glasser NF, Nienow P, Mair D. 2005b. The structural glaciology of a temperate valley glacier: Haut Glacier d'Arolla, Valais, Switzerland. *Arctic Antarctic and Alpine Research* **37**(2): 218–232.

Google Earth 7.0.3.8542. 2013. Vadrec del Forno 46°17′N to 46°20′N, 9°40′E to 9°43′E. Available through: http://www.google.com/earth/index.html. [Accessed 15 May 2013].

Hambrey MJ. 1977a. Foliation, minor folds and strain in glacier ice. *Tectonophysics* **39**: 397–416.

Hambrey MJ. 1977b. Supraglacial drainage and its relationship to structure with particular reference to Charles Rabots Bre, Okstindan, Norway. *Norsk Geogrrafisk Tidsskrift* **31**: 69–77.

Hambrey MJ, Glasser NF. 2003a. Glacial sediments: processes, environments and facies. In *Encyclopedia of Sediments and Sedimentary Rocks*, Middleton GV (ed). Dordrecht: Kluwer; 316–331.

Hambrey MJ, Glasser NF. 2003b. The role of folding and foliation development in the genesis of medial moraines: examples from Svalbard glaciers. *The Journal of Geology* **111**(4): 471–485.

Hambrey MJ, Lawson W. 2000. Structural styles and deformation fields in glaciers: a review. In *Deformation of Glacial Materials*, Maltman

AJ, Hubbard B, Hambrey MJ (eds). Geological Society London Special Publications **176**: 59–83.

Hambrey MJ, Milnes AG. 1977. Structural geology of an Alpine glacier (Griesgletscher, Valais, Switzerland). *Eclogae Geologicae Helvetiae* **70**: 667– 684.

Hambrey MJ, Müller F. 1978. Structures and ice deformation in the White Glacier, Axel Heiberg Island, Northwest Territories, Canada. *Journal of Glaciology* **20**: 41–66.

Hambrey MJ, Dowdeswell JA, Murray T, Porter PR. 1996. Thrusting and debris- entrainment in a surging glacier, Bakaninbreen, Svalbard. *Annals of Glaciology* **22**: 241–248.

Hambrey MJ, Bennett MR, Dowdeswell JA, Glasser NF, Huddart D. 1999. Debris entrainment and transfer in polythermal valley glaciers. *Journal of Glaciology* **45**(149): 69–86.

Hambrey MJ, Murray T, Glasser NF, Hubbard A, Hubbard B, Stuart G, Hansen S, Kohler J. 2005. Structure and changing dynamics of a polythermal valley glacier on a centennial timescale: Midre Lovenbreen, Svalbard. *Journal of Geophysical Research* **110**: F01006. DOI: 10.1029/2004JR000128.

Harper JT, Humphrey NF, Pfeffer WT. 1998. Crevasse patterns and the strain-rate tensor: a high-resolution comparison. *Journal of Glaciology* **44**(146): 68–76.

Hobbs BE, Means WD, Williams PF. 1976. *An Outline of Structural Geology*. John Wiley and Sons: Chichester.

Hooke RLeB, Hudleston PJ. 1978. Origin of foliation in glaciers. *Journal of Glaciology* **20**(83): 285–299.

Hubbard B, Glasser NF. 2005. *Field Techniques in Glaciology and Glacial Geomorphology*. John Wiley and Sons Ltd: Chichester.

Hubbard B, Glasser NF, Hambrey MJ, Etienne J. 2004. A sedimentological and isotopic study of the origin of supraglacial debris bands: Kongsfjorden, Svalbard. *Journal of Glaciology* **50**: 157–170.

Jansson P, Näslund J-O, Pettersson R, Richardson- Näslund C, Holmlund P. 2000. Debris entrainment and polythermal structure in the terminus of Storglaciären. In *Debris-Covered Glaciers*, Nakawo M, Raymond CF, Fountain A (eds). *Proceedings of a workshop held at Seattle, September 2000*. IAHS Publication **264**: 143–151.

Kirkbride MP. 1995. Processes of transportation. In *Modern Glacial Environments: Processes, Dynamics and Sediments. Vol. 1. Glacial Environments*, Menzies J (ed). Butterworth-Heinemann: Oxford.

Kirkbride M, Spedding N. 1996. The influence of englacial drainage on sediment- transport pathways and till texture of temperate valley glaciers. *Annals of Glaciology* **22**: 160–166.

Krenek LO. 1958. The formation of dirt cones on Mount Ruapehu, New Zealand. *Journal of Glaciology* **3**(24): 312–314.

Lawson WJ, Sharp MJ, Hambrey MJ. 1994. The structural geology of a surge-type glacier. *Journal of Structural Geology* **16**(10): 1447–1462.

Mair D, Willis I, Fischer UH, Hubbard B, Nienow P, Hubbard A. 2003. Hydrological controls on patterns of surface, internal and basal motion during three 'spring events': Haut Glacier d'Arolla, Switzerland. *Journal of Glaciology* **49**(167): 555–567.

Meier MF. 1960. Mode of flow of Saskatchewan Glacier, Alberta, Canada. US Geological Survey Professional Paper 351.

Moncrieff ACM. 1989. Classification of poorly-sorted sedimentary-rocks. *Sedimentary Geology* **65**: 191–194.

Nath PC, Vaughan DG. 2003. Subsurface crevasse formation in glaciers and ice sheets. *Journal of Geophysical Research* **108**(B1): 2020. DOI: 10.1029/2001JB000453.

Nye JF. 1952. The mechanics of glacier flow. *Journal of Glaciology* **2**: 82–93.

Oerlemans J, Giesen RH, Van Den Broeke MR. 2009. Retreating alpine glaciers: increased melt rates due to accumulation of dust (Vadret da Morteratsch, Switzerland). *Journal of Glaciology* **55**(192): 729–736.

Powers MC. 1953. A new roundness scale for sedimentary particles. *Journal of Sedimentary Petrology* **23**(2): 117–119.

Roberson S. 2008. Structural composition and sediment transfer in a composite cirque glacier: glacier de St. Sorlin, France. *Earth Surface Processes and Landforms* **33**: 1931–1947.

Small RJ. 1987. Englacial and supraglacial sediment: transport and deposition. In *Glaciofluvial Sediment Transfer: An Alpine Perspective*, Gurnell AM, Clark MJ. (eds). Wiley: Chichester. Q1

Small RJ, Clarke MJ, Cawse TJP. 1979. The formation of medial moraines on Alpine glaciers. *Journal of Glaciology* **22**: 43–52.

Stenborg T. 1968. Glacier drainage connected with ice structures. *Geografiska Annaler* **50**(A): 25–53.

Swiss Glacier Monitoring Network. 2013. Glaciological reports (1881-2009) 'The Swiss Glaciers', Yearbooks of the Cryosheric Commission of the Swiss Academy of Sciences (SCNAT) published since 1964 by the Laboratory of Hydraulics and Glaciology (VAW) of ETH Zurich. No 1-126 (http://glaziology.ethz.ch/swiss-glaciers/).

Switzerland Mobility. 2013. Vadrec del Forno 46°17′N to 46°20′N, 9°40′E to 9°43′E. Available through: http://www.schweizmobil.ch/en/schweizmobil.html. [Accessed 21 May 2013].

Trommsdorff V, Connolly JAD. 1996. The ultramafic contact aureole about the Bregaglia (Bergell) tonalite: isograds and a thermal model. *Schweizerische Mineralogische und Petrographische Mitteilungen* **76**: 537–547.

Wadham JL, Nuttall A. 2002. Multiphase formation of superimposed ice during a mass-balance year at a maritime high-Arctic glacier. *Journal of Glaciology* **48**(163): 545–551.

Author Query Form

Journal: Earth Surface Processes and Landforms

Article: esp_3521

Dear Author,

During the copyediting of your paper, the following queries arose. Please respond to these by annotating your proofs with the necessary changes/additions.

- If you intend to annotate your proof electronically, please refer to the E-annotation guidelines.
- If you intend to annotate your proof by means of hard-copy mark-up, please refer to the proof mark-up symbols guidelines. If manually writing corrections on your proof and returning it by fax, do not write too close to the edge of the paper. Please remember that illegible mark-ups may delay publication.

Whether you opt for hard-copy or electronic annotation of your proofs, we recommend that you provide additional clarification of answers to queries by entering your answers on the query sheet, in addition to the text mark-up.

Query No.	Query	Remark
Q1	AUTHOR: Reference Small Rj. 1987 has not been cited in the text. Please indicate where it should be cited; or delete from the Reference List.	
Q2	AUTHOR: Figure 7 contains small and poor quality of texts and has been saved at a low resolution of 300 dpi. Please check and provide replacement figure/s with better quality.	

WILEY-BLACKWELL

USING e-ANNOTATION TOOLS FOR ELECTRONIC PROOF CORRECTION

Required software to e-Annotate PDFs: Adobe Acrobat Professional or Adobe Reader (version 7.0 or above). (Note that this document uses screenshots from Adobe Reader X)
The latest version of Acrobat Reader can be downloaded for free at: http://get.adobe.com/uk/reader/

Once you have Acrobat Reader open on your computer, click on the Comment tab at the right of the toolbar:

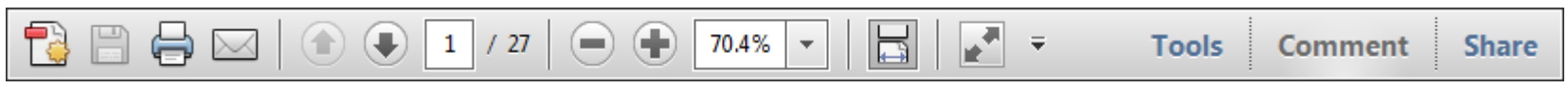

This will open up a panel down the right side of the document. The majority of tools you will use for annotating your proof will be in the Annotations section, pictured opposite. We've picked out some of these tools below:

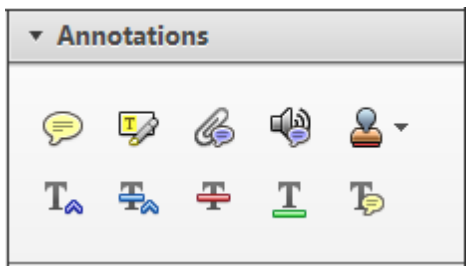

1. Replace (Ins) Tool – for replacing text.

Strikes a line through text and opens up a text box where replacement text can be entered.

How to use it

- Highlight a word or sentence.
- Click on the Replace (Ins) icon in the Annotations section.
- Type the replacement text into the blue box that appears.

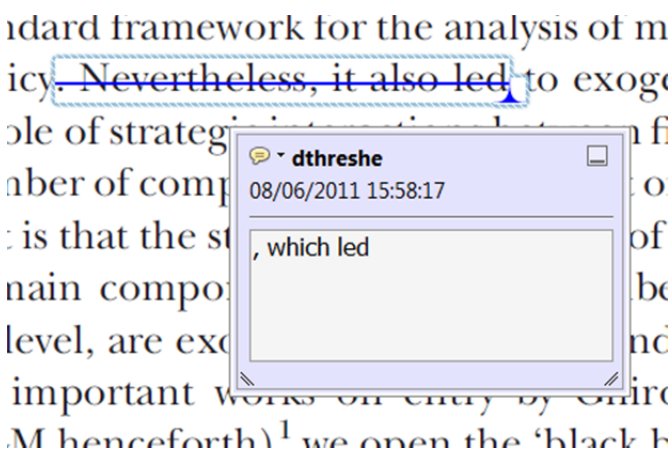

2. Strikethrough (Del) Tool – for deleting text.

Strikes a red line through text that is to be deleted.

How to use it

- Highlight a word or sentence.
- Click on the Strikethrough (Del) icon in the Annotations section.

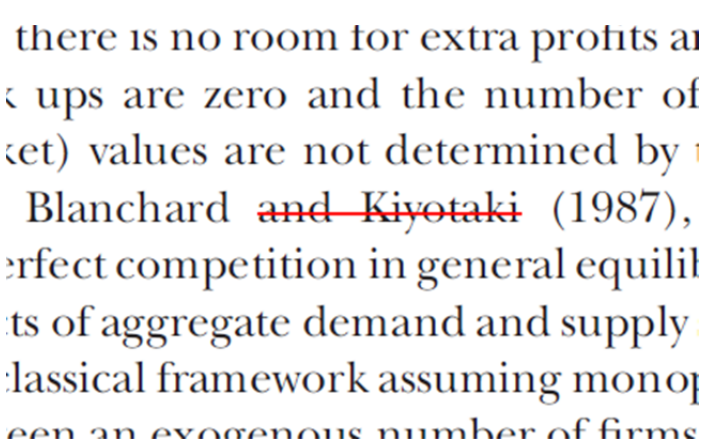

3. Add note to text Tool – for highlighting a section to be changed to bold or italic.

Highlights text in yellow and opens up a text box where comments can be entered.

How to use it

- Highlight the relevant section of text.
- Click on the Add note to text icon in the Annotations section.
- Type instruction on what should be changed regarding the text into the yellow box that appears.

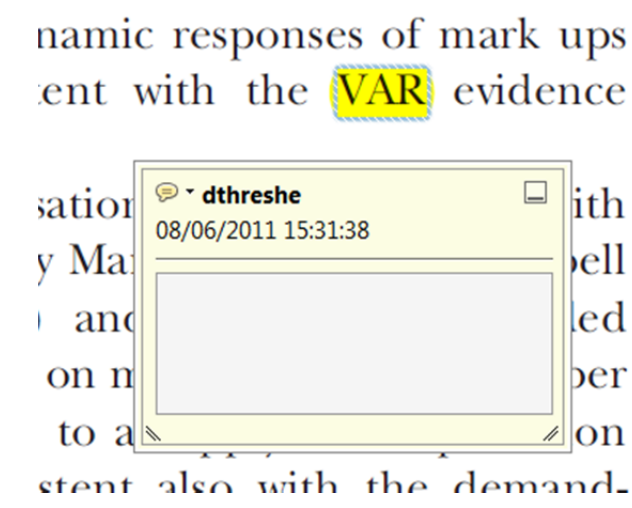

4. Add sticky note Tool – for making notes at specific points in the text.

Marks a point in the proof where a comment needs to be highlighted.

How to use it

- Click on the Add sticky note icon in the Annotations section.
- Click at the point in the proof where the comment should be inserted.
- Type the comment into the yellow box that appears.

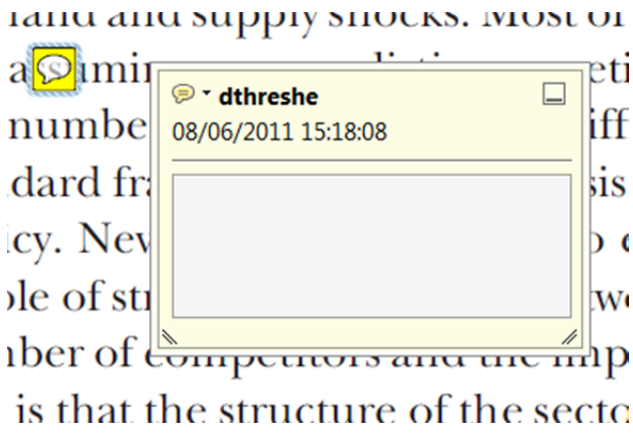

WILEY-BLACKWELL

USING e-ANNOTATION TOOLS FOR ELECTRONIC PROOF CORRECTION

5. Attach File Tool – for inserting large amounts of text or replacement figures.

Inserts an icon linking to the attached file in the appropriate pace in the text.

How to use it

- Click on the Attach File icon in the Annotations section.
- Click on the proof to where you'd like the attached file to be linked.
- Select the file to be attached from your computer or network.
- Select the colour and type of icon that will appear in the proof. Click OK.

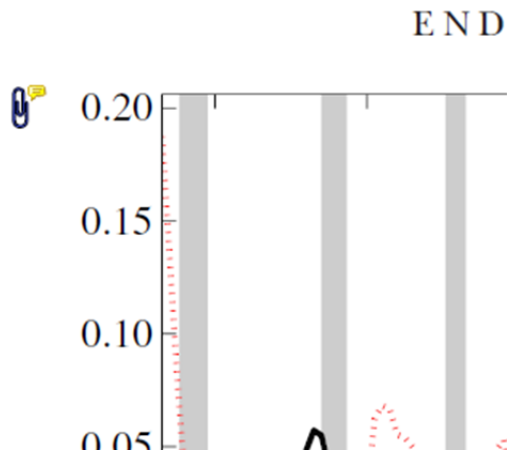

6. Add stamp Tool – for approving a proof if no corrections are required.

Inserts a selected stamp onto an appropriate place in the proof.

How to use it

- Click on the Add stamp icon in the Annotations section.
- Select the stamp you want to use. (The Approved stamp is usually available directly in the menu that appears).
- Click on the proof where you'd like the stamp to appear. (Where a proof is to be approved as it is, this would normally be on the first page).

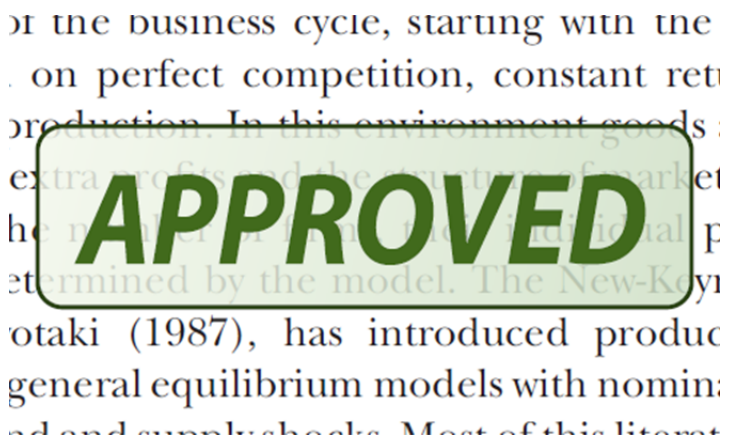

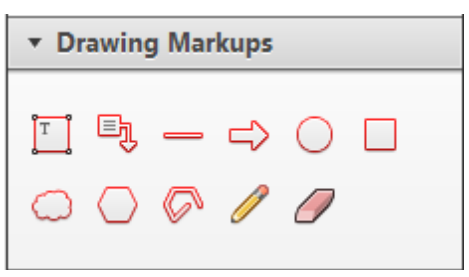

7. Drawing Markups Tools – for drawing shapes, lines and freeform annotations on proofs and commenting on these marks.

Allows shapes, lines and freeform annotations to be drawn on proofs and for comment to be made on these marks..

How to use it

- Click on one of the shapes in the Drawing Markups section.
- Click on the proof at the relevant point and draw the selected shape with the cursor.
- To add a comment to the drawn shape, move the cursor over the shape until an arrowhead appears.
- Double click on the shape and type any text in the red box that appears.

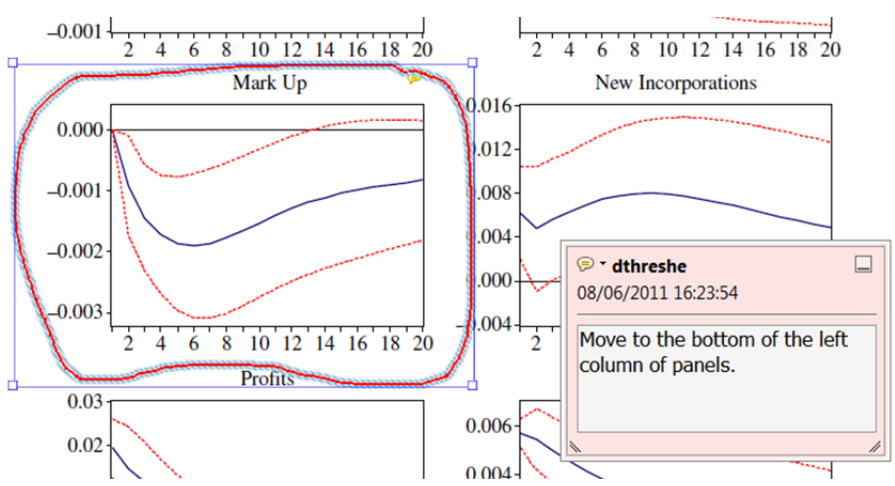

For further information on how to annotate proofs, click on the Help menu to reveal a list of further options: